Analytical Biochemistry 645 (2022) 114634

Contents lists available at ScienceDirect

Analytical Biochemistry

journal homepage: www.elsevier.com/locate/yabio

Ultrasensitive colorimetric detection of amoxicillin based on Tris-HCl-induced aggregation of gold nanoparticles

Duy Khiem Nguyen [a], Chang-Hyun Jang [a,*]

[a] Department of Chemistry, Gachon University, Seongnam-daero 1342, Sujeong-gu, Seongnam-si, Gyeonggi-do, 13120, Republic of Korea

ARTICLE INFO

Keywords:
Colorimetric aptasensors
DNA aptamer
UV–Vis absorbance
Gold nanoparticles
Amoxicillin

ABSTRACT

An ultrasensitive colorimetric aptasensor for the detection of amoxicillin (AMO) based on the Tris-HCl buffer-induced aggregation of gold nanoparticles (AuNPs) was developed. The AuNPs were aggregated by the addition of Tris-HCl buffer. The adsorption of the aptamer on the AuNP surface increased its negative charge density, leading to the enhancement of the electrostatic repulsion between the nanoparticles, thus protecting AuNPs from aggregation in the Tris-HCl buffer. However, the specific binding of the aptamer with AMO induced conformational changes in the aptamer, which reduced the adsorption of the aptamer on the AuNP surface, diminishing the protective effect of the aptamer. This resulted in the aggregation of AuNPs by Tris-HCl buffer, and consequently, color change of the solution containing AuNPs from red to blue. Under optimized conditions, a linear relationship between the absorbance ratio variation ($\Delta A_{680}/A_{520}$) and the AMO concentration was observed in the concentration range of 0.1–125 nM, with a detection limit of 67 pM. The developed biosensor exhibited high selectivity toward AMO. Moreover, this strategy was successfully applied to the detection of AMO in lake water samples. Thus, the present aptasensor is a promising alternative for the simple and ultrasensitive detection of AMO in the environment.

1. Introduction

Amoxicillin (AMO) is a β-lactam antibiotic extensively used for treating various bacterial infections in humans and animals by inhibiting the growth of or killing both gram-negative and gram-positive bacteria [1–4]. However, the overuse of AMO in food-producing animals can lead to the presence of residues in food and water sources, which can cause unpleasant side effects in humans, such as hypersensitivity, nausea, diarrhea, and dermatitis [2,5]. The residue of AMO can also contribute to the emergence of antibiotic resistance in bacteria [1,6]. Thus, the monitoring and quantification of AMO in aqueous environments at low concentrations is an important application.

Existing techniques for AMO detection include surface plasmon resonance [3,6], chromatography [1,7], electrochemistry [4,8,9], and fluorescence [10]. However, these techniques have several limitations mainly related to the requirement of sophisticated and expensive equipment, complex sample preparation, and time-consuming procedures [11]. Thus, it is necessary to develop simple, cost-effective, and precise alternatives without using sophisticated instruments for the detection of AMO.

Recently, aptamer-based colorimetric biosensing assays have been developed and widely applied to detect various target molecules because of their simplicity, low cost, high sensitivity, and specific detection without the requirement of sophisticated instruments [12]. In these assays, gold nanoparticles (AuNPs) are extensively used as colorimetric probes because of their excellent optical properties and the ability to absorb aptamers (single-stranded DNA or RNA) through electrostatic and non-covalent interactions [13,14]. The aggregation of AuNPs increases the size of particles in solution, which affects the wavelength of light absorbed by the nanoparticles, resulting in remarkable color changes of the solution from wine-red (dispersed state) to purple or blue (aggregated state) [12,15,16]. In addition to AuNPs, aptamers are commonly used as recognition elements that improve the specificity of biosensors owing to their ability to bind target molecules with high affinity and specificity [17,18]. The unfolded aptamers can easily adsorb onto the surface of negatively charged AuNPs via their exposed nucleobases, thus protecting the AuNPs from salt-induced aggregation by enhancing electrostatic repulsion between the nanoparticles [16]. However, the interaction of the aptamers with their respective ligands induces conformational changes in the aptamers,

* Corresponding author.
E-mail address: chjang4u@gachon.ac.kr (C.-H. Jang).

https://doi.org/10.1016/j.ab.2022.114634
Received 20 December 2021; Received in revised form 15 February 2022; Accepted 28 February 2022
Available online 8 March 2022

leading to poor adsorption on the surface of AuNPs, resulting in the aggregation of AuNPs under high-salt concentration; thus, the color of the nanoparticle solution changes from wine-red to purple/blue [19,20].

In various reported colorimetric biosensors, a high-concentration solution of salt (e.g., sodium chloride) is commonly used to aggregate AuNPs [19,21–23]. However, biosensors based on the salt-induced aggregation of AuNPs are susceptible to the sensing environment (e.g., acidity) and may suffer from time-consuming and false-positive signal readouts and higher detection limits [15,24,25]. In this study, we exploited the application of a Tris-HCl buffer solution for the aggregation of AuNPs and aimed to develop a novel colorimetric platform for AMO detection based on aptamers, AuNPs, and a Tris-HCl buffer instead of a high-salt concentration solution. Neutral Tris molecules can easily displace anionic citrate ions on the AuNP surface because of the strong coordination interactions between the nitrogen atoms on the Tris molecules and AuNPs, which greatly reduces the electrostatic repulsion force between nanoparticles, resulting in the aggregation of AuNPs [26,27]. The use of Tris-HCl buffer offers significant advantages not only in the aggregation of AuNPs, but also in controlling the pH of the solutions. As illustrated in Scheme 1, the AMO-specific aptamer can adsorb onto the surface of citrate-capped AuNPs via coordination interactions and protect AuNPs from aggregation in the Tris-HCl buffer solution; thus, the AuNPs maintain their dispersion state and remain wine-red. However, in the presence of AMO, the specific interactions of the aptamer with AMO induce a conformational change in the aptamers, which reduces the adsorption of the aptamer on the surface of the AuNPs. Owing to the loss of the protective effect of the aptamer, AuNPs are easily aggregated after the addition of Tris-HCl buffer solution. Accordingly, the color of AuNPs changes from wine-red to blue, which can be easily observed by the naked eye. By measuring the color and absorption change of the AuNP solution, the concentration of AMO can be easily quantified. Our results indicate that the proposed sensor is simple, inexpensive, easy to operate, and highly sensitive and selective for the detection of AMO without the requirement of any kind of sophisticated instrumentation. Moreover, this method was successfully applied to the quantitative detection of AMO in potential application environments, for example, lake water samples, with satisfactory results.

2. Materials and methods

2.1. Chemicals and apparatus

The reagents, materials, and apparatus used in this study are listed in the Supplementary Material.

2.2. Synthesis of gold nanoparticles

Citrate-capped AuNPs (~13 nm in diameter) were synthesized by the citrate reduction method according to a previously reported protocol [28]. Briefly, 50 mL of trisodium citrate (38.8 mM) was quickly added to a boiling $HAuCl_4$ solution (500 mL, 1 mM) under vigorous stirring and the mixture was boiled for 20 min. Subsequently, the heater was removed, and stirring was continued until the solution cooled to room temperature. The resulting wine-red solution was centrifuged at 7000 rpm for 10 min to remove the aggregated particles. The obtained AuNP solution was stored in a brown glass bottle at 4 °C before use. The

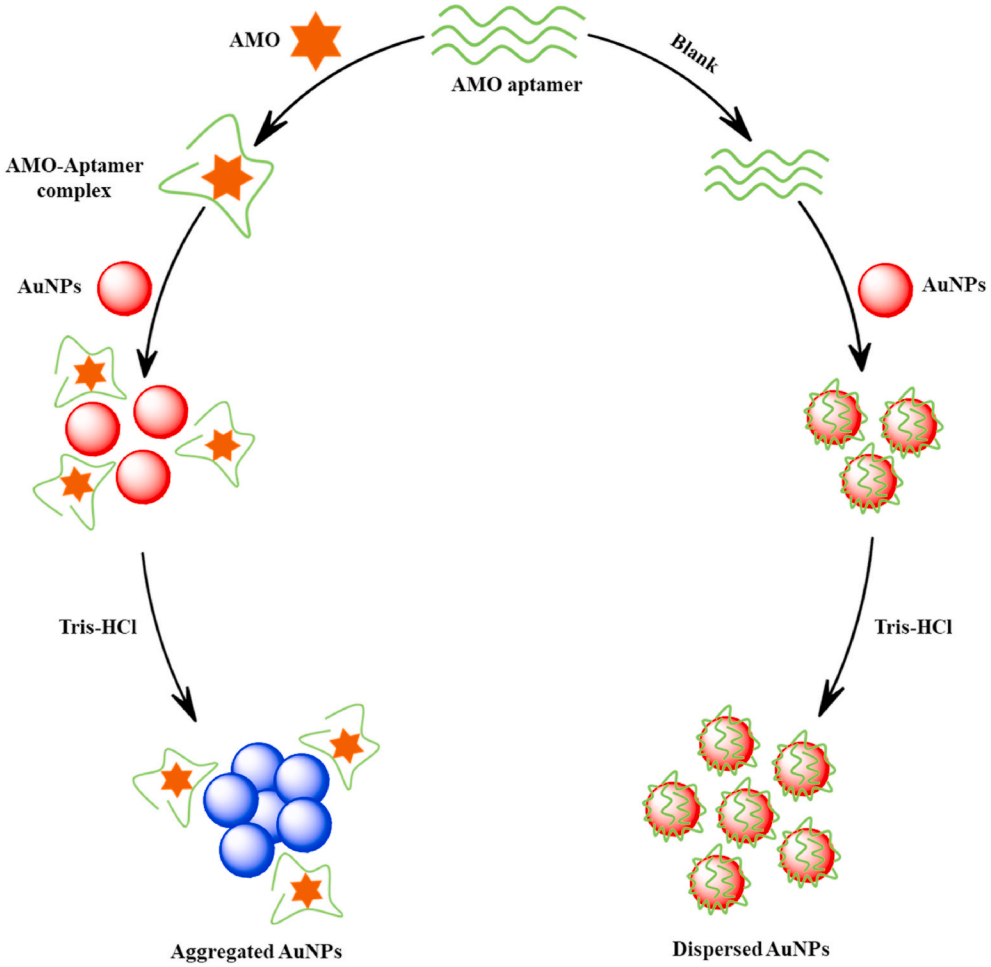

Scheme 1. Schematic illustration of the colorimetric strategy for amoxicillin (AMO) detection based on Tris-HCl-induced aggregation of gold nanoparticles (AuNPs).

concentration of the prepared AuNP solution was calculated to be 4 nM using ultraviolet–visible (UV–vis) spectroscopy, according to previous publications [13,22].

2.3. Fluorescence assays

To evaluate the effect of AMO on the adsorption of aptamer on the AuNPs, 50 μL of FAM-aptamer (40 nM, in 10 mM phosphate buffer, pH 7.4) was incubated with 50 μL of AMO of various concentrations at 37 °C for 30 min. Then, 100 μL of AuNPs was added and incubated at 25 °C for another 2 h. The mixtures were centrifuged (14000 rpm, 15 min) and washed with phosphate buffer (PB, pH 7.4) three times to remove the nonadsorbed FAM-aptamer. Finally, the mixtures were dissolved in 200 μL PB (pH 7.4) containing 10 mM KCN. The fluorescence of the FAM-aptamer was measured by excitation at 470 nm using a microplate reader (Synergy H1, Biotek, USA).

2.4. Optimization of detection conditions

Various experimental conditions, including the concentration of Tris-HCl, the aggregation time of AuNPs in Tris-HCl solution, the effect of pH value of Tris-HCl solution, the concentration of AMO-specific aptamer, the incubation time of aptamer with AuNPs, and the incubation time of aptamer with AMO, were optimized to identify the optimal conditions for developing an ultrasensitive colorimetric aptasensor for AMO detection. Details of the experimental procedures are provided in the Supplementary Material.

2.5. Procedure for AMO detection

As in a typical experiment, 50 μL of aptamer was mixed with 50 μL of AMO solution in a 1.5 mL centrifuge tube, and the mixtures were incubated at 37 °C for 30 min. Then, 650 μL of AuNPs was added to a centrifuge tube, mixed well, and incubated for another 2 h at 25 °C. Finally, 750 μL of 40 mM Tris-HCl (pH 7) was added and incubated for 30 min at 25 °C. The final concentration of the aptamer was 40 nM. The final concentrations of AMO were 0, 0.1, 1, 5, 10, 25, 50, 75, 100, 125, 150, 175, and 250 nM. The resulting solutions were transferred to a quartz cell, and the absorbance spectra of each solution were recorded at 520 nm (A_{520}) and 680 nm (A_{680}). Then, the absorbance ratio variation, $\Delta A_{680}/A_{520}$, was calculated ($\Delta A_{680}/A_{520}$ = the absorbance ratio (A_{680}/A_{520}) in the presence of AMO – the absorbance ratio (A_{680}/A_{520}) in the absence of AMO).

2.6. Selectivity test

To investigate the selectivity of the developed colorimetric aptasensor for AMO detection, common interfering substances, such as sulfamethazine sodium salt (SMT), sulfamethoxazole (SMXZ), trimethoprim (TMP), tetracycline hydrochloride (TET), chloramphenicol (CLP), norfloxacin (NFX), sulfamethizole (SMZ), ampicillin (AMP), penicillin G (PEC), calcium chloride ($CaCl_2$), magnesium chloride ($MgCl_2$), and potassium chloride (KCl), were added to the solutions and tested under the same optimal conditions. The concentration of AMO was maintained at 100 nM, while that of the interfering substances was 1 μM.

3. Results and discussion

3.1. Feasibility of the colorimetric assay for AMO detection

To prove the feasibility of the proposed aptasensor for the detection of AMO, the UV–vis absorption spectra and the color change of AuNP solutions after treatment with different substances were studied. As shown in Fig. 1A and B, the prepared solution of AuNPs was red and had a strong characteristic absorbance peak at 520 nm, demonstrating that

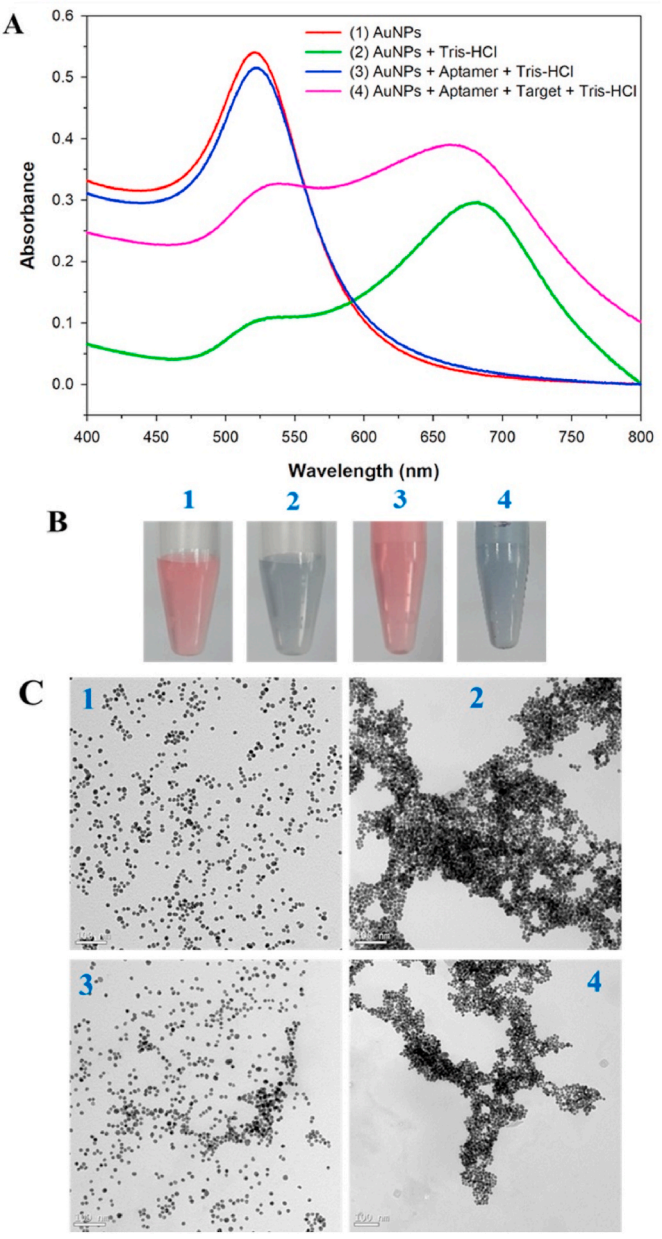

Fig. 1. UV–visible absorption spectra (A), visual color changes (B), and transmission electron microscopy (TEM) images (C) of gold nanoparticle (AuNP) solutions after mixing and incubating with different substances: (1) AuNPs, (2) AuNPs + Tris-HCl, (3) AuNPs + aptamer + Tris-HCl, and (4) AuNPs + aptamer + amoxicillin (AMO) + Tris-HCl. Experimental conditions: concentration $(C)_{AuNPs}$ = 4 nM, $C_{aptamer}$ = 40 nM, $C_{Tris\text{-}HCl}$ = 20 mM, C_{AMO} = 100 nM. (For interpretation of the references to color in this figure legend, the reader is referred to the Web version of this article.)

the AuNPs were highly dispersed (sample 1). This was due to the electrostatic repulsion produced by the negative charges of the citrate layer that was weakly adsorbed on the surface of AuNPs, which enhanced the stability of AuNPs in an aqueous solution [12,29]. Upon the addition of Tris-HCl, a red-to-blue color change was observed, and the absorbance peak at 520 nm (representing the dispersed AuNPs) dramatically decreased, while a new peak appeared at 680 nm (representing the aggregated AuNPs), implying that the AuNPs had aggregated (sample 2). This was because the displacement of anionic citrate ions on the AuNP surface by neutral Tris reduced the electrostatic repulsion force between the nanoparticles, resulting in the aggregation of AuNPs [26,27]. When the AMO-specific aptamer was added, the color of the AuNP

solution was still red and only one absorbance peak at 520 nm was observed with an intensity almost as high as that of free AuNPs, demonstrating that the AuNPs were still dispersed (sample 3). This was due to the adsorption of the aptamer on the AuNP surface, which increased the negative charge density on the AuNP surface, enhancing the electrostatic repulsion between the nanoparticles, and thus protecting AuNPs from aggregation in Tris-HCl buffer solution [16,20,30]. However, after adding both AMO-specific aptamer and AMO, the solution changed from red to blue, and the absorbance at 520 nm dramatically decreased, while the absorbance at 680 nm clearly increased, indicating the aggregation of AuNPs (sample 4). This was because the specific binding of the aptamer with AMO induced conformational changes in the aptamer, which reduced the adsorption of the aptamer on the AuNP surface, diminishing the protective effect of the aptamer, and finally resulting in aggregation of AuNPs [1,19,20]. Accordingly, the color of the solution changed from red to blue.

These results were further confirmed by transmission electron spectroscopy (TEM; Fig. 1C). The prepared AuNPs had a spherical morphology with a mean diameter of 13 nm and were monodispersed in the solution (sample 1 in Fig. 1C). The addition of Tris-HCl buffer solution caused the complete aggregation of AuNPs (sample 2 in Fig. 1C). In the presence of the aptamer, the AuNPs aggregated slightly after incubation with Tris-HCl (sample 3 in Fig. 1C). However, in the presence of both aptamer and AMO, obvious aggregation of AuNPs was observed after the addition of Tris-HCl (sample 4 in Fig. 1C). These results are consistent with the results obtained from UV–vis absorption spectra.

The effect of AMO on the reduced aptamer adsorption on the AuNPs was further evaluated. Here, the aptamer was labeled by carboxyfluorescein (FAM). We first incubated FAM-aptamer with AMO and then added AuNPs. After washing away the nonadsorbed aptamer, KCN was added to dissolve the AuNPs and release the adsorbed aptamer for fluorescence quantification. The total adsorbed FAM-aptamer on the AuNPs was calculated according to the standard curve (Fig. S1, Supplementary Material). The results clearly showed that the adsorbed aptamer decreased as the concentration of AMO increased (Fig. 2). Therefore, the reduced aptamer adsorption on the AuNPs may have resulted from the specific binding of the aptamer with AMO.

3.2. Optimization of the detection conditions

The reaction conditions strongly affect the performance of the biosensors. Thus, to achieve the best sensing performance of the proposed colorimetric assay for AMO detection, several experimental conditions, including the concentration of Tris-HCl, the incubation time of AuNPs with Tris-HCl, the pH value of the Tris-HCl solution, the concentration of AMO-specific aptamer, the incubation time of aptamer with AuNPs, and the incubation time of aptamer with AMO, were optimized. The value of A_{680}/A_{520} was selected to investigate the aggregation state of the AuNPs. The higher the value of A_{680}/A_{520}, the higher was the degree of aggregation of the AuNPs. The respective data and figures are provided in the Supplementary Material. After optimization, we found that the best conditions for developing a sensitive colorimetric assay for AMO detection were a Tris-HCl concentration of 20 mM (Fig. S2), an incubation time of AuNPs with Tris-HCl of 30 min (Fig. S3), a pH value of 7.4 (Fig. S4), an AMO-specific aptamer of 40 nM (Fig. S5), an incubation time of aptamer with AuNPs of 2 h (Fig. S6), and an incubation time of aptamer with AMO of 30 min (Fig. S7).

3.3. Sensitivity and selectivity of the colorimetric assay for AMO detection

Under the optimal experimental conditions, the proposed colorimetric aptasensor was applied to investigate the relationship between the absorbance ratio variation and AMO concentration in the range of 0.1–250 nM. As presented in Fig. 3A, the absorbance at 520 nm gradually decreased, while the absorbance at 680 nm gradually increased with increasing AMO concentration, and the color of the corresponding AuNP solutions gradually changed from red to purple and blue (inset of Fig. 3A). The absorbance ratio variation ($\Delta A_{680}/A_{520}$) was linearly proportional to the concentration of AMO (C_{AMO}) over the concentration range of 0.1 nM–125 nM (Fig. 3B). The linear regression equation was $\Delta A_{680}/A_{520} = 0.01175\ C_{AMO} + 0.15996$ with a linear correlation coefficient (R^2) of 0.9912. The limit of detection (LOD) was calculated to be 67 pM using formula 3σ/slope [17,30]. However, when the concentration of AMO was more than 125 nM, the $\Delta A_{680}/A_{520}$ tended to saturate (Fig. S8). Compared to other existing techniques for the detection of AMO such as photoluminescence, high-performance liquid chromatography, electrochemistry, fluorescence, and liquid crystal-based aptasensor, our proposed colorimetric assay exhibits a wider linear range and a lower LOD, as summarized in Table 1.

In addition to sensitivity, selectivity is an important parameter of the biosensor; thus, the selectivity of the proposed colorimetric aptasensor for AMO detection was also investigated. To test selectivity, AMO and other common interfering substances such as SMT, SMXZ, TMP, TET, CLP, NFX, SMZ, AMP, PEC, K^+, Ca^{2+}, Mg^{2+}, were added to the sensing solutions under the same optimized experimental conditions. The concentration of AMO was maintained at 100 nM, while that of the interfering substances was 1 μM. The absorption spectra of the solutions were recorded, and the absorbance ratio variation ($\Delta A_{680}/A_{520}$) was then calculated. As illustrated in Fig. 4A, only the solution containing AMO changed color from red to blue, while solutions containing other interferents remained red. Moreover, as shown in Fig. 4B, a significant change in the $\Delta A_{680}/A_{520}$ ratio of the solution with added AMO, and a negligible change in the solutions with other interferents were observed. These results demonstrate that the proposed aptasensor has excellent selectivity toward AMO, which can be attributed to the highly specific binding of AMO aptamers to AMO.

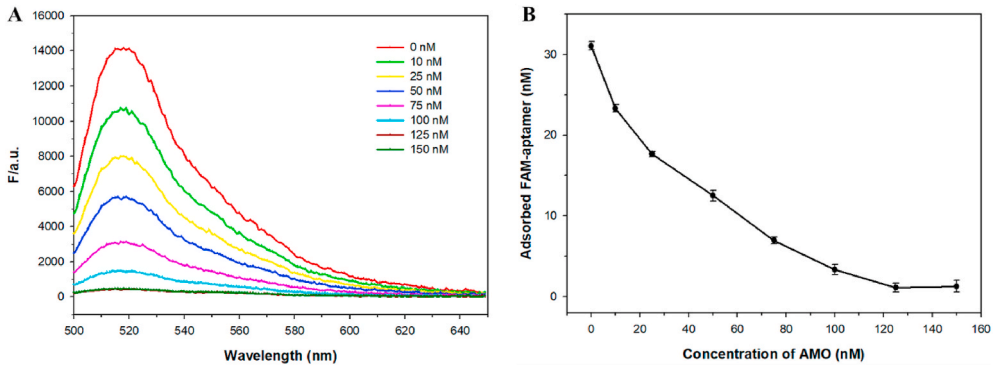

Fig. 2. (A) Fluorescence spectra of adsorbed FAM-aptamer on the AuNPs prepared in the presence of various concentrations of amoxicillin (AMO). (B) Relationship between adsorbed FAM-aptamer and AMO concentrations.

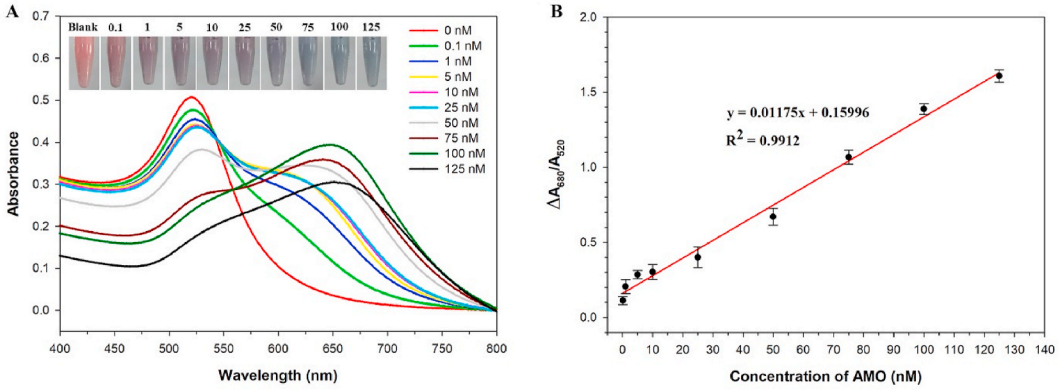

Fig. 3. (A) The UV–visible absorption spectra of the gold nanoparticle (AuNP) solutions in the presence of mixtures of 40 nM aptamer and various concentrations of amoxicillin (AMO). (B) Linear calibration curve showing the variation of absorbance ratio ($\Delta A_{680}/A_{520}$) versus concentration of AMO. Inset shows the visible color changes of the corresponding AuNP solutions. (For interpretation of the references to color in this figure legend, the reader is referred to the Web version of this article.)

Table 1
Comparison of the proposed aptamer-based colorimetric assay with other existing techniques for amoxicillin detection.

Techniques	Linear range	LOD	Reference
Photoluminescence	0.547–163.8 μM	0.383 nM	[2]
Electrochemistry	0.5–3 nM	200 pM	[5]
Chemosensor	100 pM–8 μM	73 pM	[6]
High-performance liquid chromatography	0.137–1368 μM	43.8 nM	[7]
Electrochemistry	0.9–69 μM	50 nM	[8]
Fluorescence	1.43–429.12 μM	825 nM	[10]
Qt AgNPs-based colorimetry[a]	10–95 μM	4.46 μM	[11]
Liquid crystal-based aptasensor	10–800 nM	3.5 nM	[31]
Colorimetric aptasensor	0.1–125 nM	67 pM	This work

[a] Qt AgNPs, quercetagetin coated silver nanoparticles.

3.4. Analysis of AMO in actual samples

The applicability of the developed colorimetric aptasensor for the detection of AMO in real samples was evaluated. Natural water sample was collected from a local lake (Shin Dae Lake, Suwon City, Republic of Korea) and filtered through a 0.22 μm membrane filter. Four different AMO concentrations were spiked into the samples, followed by analysis using the developed colorimetric assay. The results are summarized in Table 2. The recoveries were in the range of 90.42%–109.21%, and the relative standard deviation (RSD) was between 3.83% and 7.56%. These results illustrate that the developed aptasensor has acceptable accuracy and satisfactory reproducibility, indicating its potential application for monitoring AMO in environmental water samples.

The proposed colorimetric method was validated using conventional high-performance liquid chromatography (HPLC). The spiked lake water samples were analyzed using both the developed method and HPLC. Table 2 shows a comparison of the results obtained by the two methods. These results demonstrate that there is no significant difference between the obtained results of the developed sensor and HPLC.

4. Conclusions

In summary, a simple and ultrasensitive colorimetric aptasensor for the detection of AMO was developed based on the color change of AuNPs induced by Tris-HCl buffer, which was controlled by the specific interaction between the aptamer, AuNPs, and AMO. Under the optimal experimental conditions, the relationship between the colorimetric response and AMO concentration was linear in the concentration range of 0.1–125 nM. The proposed biosensor exhibited a wide linear detection range and a low LOD of 67 pM, as well as high selectivity toward AMO than other interferents. Moreover, the developed method was successfully applied for AMO determination in real lake water samples with a high recovery. This simple and ultrasensitive colorimetric aptasensor shows great potential for AMO detection in the environment

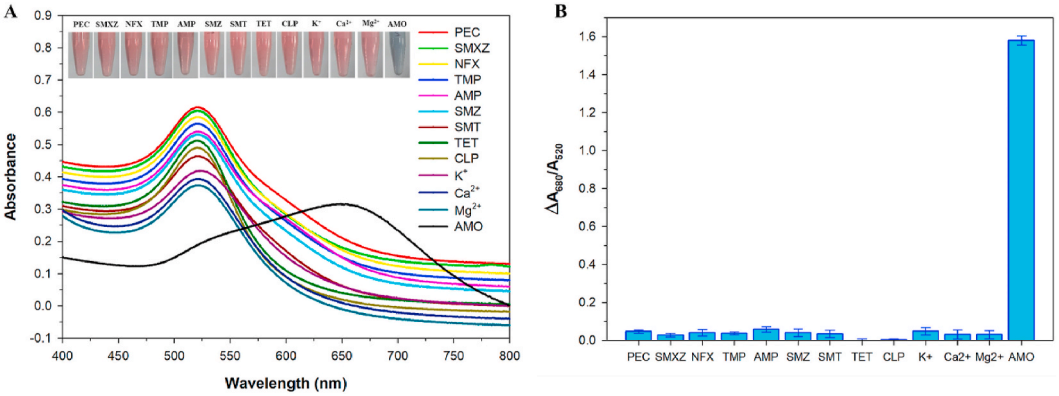

Fig. 4. Specificity of the proposed colorimetric aptasensor for amoxicillin (AMO). (A) The UV–visible absorption spectra of the gold nanoparticle (AuNP) solutions in the presence of various antibiotics and metal ions (inset: visible color changes of the corresponding AuNP solutions). (B) The absorbance ratio variation ($\Delta A_{680}/A_{520}$) of the AuNP solutions in the presence of AMO and potential interferents. The concentration of AMO was maintained at 100 nM, while that of the interfering substances was 1 μM. (For interpretation of the references to color in this figure legend, the reader is referred to the Web version of this article.)

Table 2
Analysis of amoxicillin (AMO) concentration in spiked lake water samples (n = 3).

Samples	Added AMO (nM)	Determined AMO (nM)		Recovery (%)		RSD (biosensor, %)
		Proposed method	HPLC	Proposed method	HPLC	
Lake water 1	5	4.271	4.763	90.42	95.26	7.56
Lake water 2	10	10.921	10.584	109.21	105.84	6.53
Lake water 3	75	73.528	76.705	98.037	102.27	3.83
Lake water 4	125	126.317	122.325	101.054	97.86	4.41

without requiring sophisticated instrumentation.

CRediT authorship contribution statement

Duy Khiem Nguyen: Conceptualization, Methodology, Data curation, Writing – original draft, Writing – review & editing, Visualization, Investigation. **Chang-Hyun Jang:** Conceptualization, Methodology, Funding acquisition, Supervision.

Declaration of competing interest

The authors declare no conflicts of interest.

Acknowledgment

This work was supported by the Basic Science Research Program of the National Research Foundation of Korea (NRF) funded by the Ministry of Education (NRF-2019R1A2C1003862).

Appendix A. Supplementary data

Supplementary data to this article can be found online at https://doi.org/10.1016/j.ab.2022.114634.

References

[1] L. Sun, L. Jia, X. Xie, K. Xie, J. Wang, J. Liu, L. Cui, G. Zhang, G. Dai, J. Wang, Quantitative analysis of amoxicillin, its major metabolites and ampicillin in eggs by liquid chromatography combined with electrospray ionization tandem mass spectrometry, Food Chem. 192 (2016) 313–318.
[2] K. Chullasat, P. Nurerk, P. Kanatharana, F. Davis, O. Bunkoed, A facile optosensing protocol based on molecularly imprinted polymer coated on CdTe quantum dots for highly sensitive and selective amoxicillin detection, Sensor. Actuator. B Chem. 254 (2018) 255–263.
[3] M.L. Yola, T. Eren, N. Atar, Molecular imprinted nanosensor based on surface plasmon resonance: application to the sensitive determination of amoxicillin, Sensor. Actuator. B Chem. 195 (2014) 28–35.
[4] P.K. Brahman, R.A. Dar, K.S. Pitre, Conducting polymer film based electrochemical sensor for the determination of amoxicillin in micellar media, Sensor. Actuator. B Chem. 176 (2013) 307–314.
[5] J. Song, M. Huang, N. Jiang, S. Zheng, T. Mu, L. Meng, Y. Liu, J. Liu, G. Chen, Ultrasensitive detection of amoxicillin by TiO_2-g-C_3N_4@AuNPs impedimetric aptasensor: fabrication, optimization, and mechanism, J. Hazard Mater. 391 (2020) 122024.
[6] A.G. Ayankojo, J. Reut, A. Öpik, A. Furchner, V. Syritski, Hybrid molecularly imprinted polymer for amoxicillin detection, Biosens. Bioelectron. 118 (2018) 102–107.
[7] T. Unutkan, S. Bakırdere, S. Keyf, Development of an analytical method for the determination of amoxicillin in commercial drugs and wastewater samples, and assessing its stability in simulated gastric digestion, J. Chromatogr. Sci. 56 (2018) 36–40.
[8] A. Wong, A.M. Santos, F.H. Cincotto, F.C. Moraes, O. Fatibello-Filho, M.D.P. T. Sotomayor, A new electrochemical platform based on low cost nanomaterials for sensitive detection of the amoxicillin antibiotic in different matrices, Talanta 206 (2020) 120252.
[9] N.K. Rosy, R.N. Goyal, Gold-palladium nanoparticles aided electrochemically reduced graphene oxide sensor for the simultaneous estimation of lomefloxacin and amoxicillin, Sensor. Actuator. B Chem. 243 (2017) 658–668.
[10] X. Zhang, Y. Ren, Z. Ji, J. Fan, Sensitive detection of amoxicillin in aqueous solution with novel fluorescent probes containing boron-doped carbon quantum dots, J. Mol. Liq. 311 (2020) 113278.
[11] N.U. Ain, I. Anis, F. Ahmed, M.R. Shah, S. Parveen, S. Faizi, S. Ahmed, Colorimetric detection of amoxicillin based on querecetagetin coated silver nanoparticles, Sensor. Actuator. B Chem. 265 (2018) 617–624.
[12] F. Li, Y. Feng, C. Zhao, B. Tang, Simple colorimetric sensing of trace bleomycin using unmodified gold nanoparticles, Biosens. Bioelectron. 26 (2011) 4628–4631.
[13] Y. Zheng, Y. Wang, X. Yang, Aptamer-based colorimetric biosensing of dopamine using unmodified gold nanoparticles, Sensor. Actuator. B Chem. 156 (2011) 95–99.
[14] L. Zhu, Y. Zhao, S. Yao, M. Xu, L. Yin, X. Zhaib, X. Teng, A colorimetric aptasensor for the simple and rapid detection of human papillomavirus type 16 L1 proteins, Analyst 146 (2021) 2712–2717.
[15] Y. Wu, L. Liu, S. Zhan, F. Wang, P. Zhou, Ultrasensitive aptamer biosensor for arsenic(III) detection in aqueous solution based on surfactant-induced aggregation of gold nanoparticles, Analyst 137 (2012) 4171–4178.
[16] Junli Feng, Qinchao Zhu, Yi Wang, Colorimetric detection of Gadidae species using probe-modified gold nanoparticles, Food Control 116 (2020) 107287.
[17] R. Bala, M. Kumar, K. Bansal, R.K. Sharma, N. Wangoo, Ultrasensitive aptamer biosensor for malathion detection based on cationic polymer and gold nanoparticles, Biosens. Bioelectron. 85 (2016) 445–449.
[18] D.K. Nguyen, C.H. Jang, Label-free liquid crystal-based biosensor for detection of dopamine using DNA aptamer as a recognition probe, Anal. Biochem. 605 (2020) 113807.
[19] R. Wang, R. Yu, Z. Wang, Q. Zhu, Z. Dai, A facile and sensitive colorimetric detection for RNase A activity based on target regulated protection effect on plasmonic gold nanoparticles aggregation, Sci. China Chem. 63 (2020) 860–864.
[20] L. Tan, K.G. Neoh, E.T. Kang, W.S. Choe, X. Su, Affinity analysis of DNA aptamer–peptide interactions using gold nanoparticles, Anal. Biochem. 421 (2012) 725–731.
[21] H. Wei, B. Li, J. Li, E. Wang, S. Dong, Simple and sensitive aptamer-based colorimetric sensing of protein using unmodified gold nanoparticle probes, Chem. Commun. (2007) 3735–3737.
[22] Q. Ma, Y. Wang, J. Jia, Y. Xiang, Colorimetric aptasensors for determination of tobramycin in milk and chicken eggs based on DNA and gold nanoparticles, Food Chem. 249 (2018) 98–103.
[23] A. Kasoju, N.S. Shrikrishna, D. Shahdeo, A.A. Khan, A.M. Alanazi, S. Gandhi, Microfluidic paper device for rapid detection of aflatoxin B1 using an aptamer based colorimetric assay, RSC Adv. 10 (2020) 11843.
[24] Z. Chen, T. Tan, C. Zhang, L. Yin, H. Ma, N. Ye, H. Qiang, Y. Lin, A colorimetric aptamer biosensor based on cationic polymer and gold nanoparticles for the ultrasensitive detection of thrombin, Biosens. Bioelectron. 56 (2014) 46–50.
[25] J. Xu, Y. Li, J. Bie, W. Jiang, J. Guo, Y. Luo, F. Shen, C. Sun, Colorimetric method for determination of bisphenol A based on aptamer-mediated aggregation of positively charged gold nanoparticles, Microchim. Acta 182 (2015) 2131–2138.
[26] H. Chi, B. Liu, G. Guan, Z. Zhang, M.-Y. Han, A simple, reliable and sensitive colorimetric visualization of melamine in milk by unmodified gold nanoparticles, Analyst 135 (2010) 1070–1075.
[27] J. Zhang, X. Xu, X. Yang, Role of Tris on the colorimetric recognition of anions with melamine-modified gold nanoparticle probe and the visual detection of sulfite and hypochlorite, Analyst 137 (2012) 3437–3440.
[28] J. Liu, Y. Lu, Preparation of aptamer-linked gold nanoparticle purple aggregates for colorimetric sensing of analytes, Nat. Protocol 1 (2006) 246–252.
[29] J. Zhou, Y. Li, W. Wang, Z. Lu, H. Han, J. Liu, Kanamycin adsorption on gold nanoparticles dominates its label-free colorimetric sensing with its aptamer, Langmuir 36 (2020) 11490–11498.
[30] W. Yang, Y. Wu, H. Tao, J. Zhao, H. Chen, S. Qiu, Ultrasensitive and selective colorimetric detection of acetamiprid pesticide based on the enhanced peroxidase-like activity of gold nanoparticles, Anal. Methods 9 (2017) 5484.
[31] D.K. Nguyen, C.-H. Jang, A label-free liquid crystal biosensor based on specific DNA aptamer probes for sensitive detection of amoxicillin antibiotic, Micromachines 12 (2021) 370.